JOM
https://doi.org/10.1007/s11837-024-06754-5
© 2024 The Minerals, Metals & Materials Society

An Ammonia Leaching Process for the Recovery of Value Metals from Nickel and Cobalt Slag

XINQIONG DAI,[1] XINCUN TANG,[1,2] WEIYI ZHANG,[1] and YUSHAN MA[1]

1.—College of Chemistry and Chemical Engineering, Central South University, Changsha 410083, China. 2.—e-mail: tangxincun@163.com

The rapid development of lithium-ion batteries has led to a shortage of cobalt and nickel resources. Recycling of nickel and cobalt slag can promote sustainable development and environmental protection. In this study, a reductive ammonia leaching method is proposed for the recovery of Ni and Co from nickel and cobalt slag (NCS) with high Ni and Co contents. The NCS powder was subjected to leaching reaction in $NH_3{\cdot}H_2O$ and $(NH_4)_2SO_3{\cdot}H_2O$ solutions. The thermodynamic feasibility of Co and Ni ammonia leaching was analyzed by E-pH diagrams, and Co and Ni could be leached as complexes $[Ni(NH_3)_n]^{2+}$, $[Co(NH_3)_n]^{2+}$. XPS and XRD were used to explore the physical phases of the materials and the chemical reactions occurring during the leaching process. The results showed that the efficient leaching of Ni and Co was achieved under the optimal experimental conditions, with 90.09% leaching rate of Ni and 89.24% leaching rate of Co. Kinetic analysis showed that the leaching process was controlled by diffusion. The complex leaching is selective and can simplify the purification process. This study can provide ideas for the recycling of nickel and cobalt solid waste resources such as spent batteries and slag.

INTRODUCTION

The development of sustainable energy sources and the construction of a low-carbon society have become the focus of social development as problems such as the energy crisis and environmental pollution have become more prominent.[1,2] Lithium-ion batteries, with their long cycle life, good safety performance, green environmental protection and other characteristics, have a wide range of applications and great economic value in portable electronic devices, electric vehicles, national defense and other fields.[3–5] Anode material is the key component that limits the performance of lithium-ion batteries.[6] At present, the most common cathode materials are $LiMO_2$ (M = Ni, Co, Mn), $LiMn_2O_4$, $LiFePO_4$ and $LiNi_xCo_yMn_{1-x-y}O_2$ (NCM).[7] NCM cathode materials with a layered structure have become one of the mainstream cathode materials for lithium-ion batteries due to their high energy density, good thermal stability and excellent cycling performance.[8,9]

As use of lithium-ion batteries keeps growing, the demand for Co and Ni is also increasing. However, the resources of Co and Ni in the earth's crust are limited. There will be a serious shortage of Ni and Co resources in the future, limiting the development of lithium-ion batteries.[10] On the other hand, the under-utilization of mineral resources and the accumulation of spent batteries generate a large amount of nickel and cobalt solid wastes. Xinjiang is a region with a significant copper-nickel ore resource base. In the process of separating and purifying the components of copper-nickel ore resources, the NiOOH oxidized cobalt precipitation process is employed to achieve the effect of cobalt removal ($NiOOH + Co^{2+} = CoOOH + Ni^{2+}$). This is followed by electrolysis, which generates pure Ni and Cu products. The cobalt removal process generates a large amount of nickel and cobalt slag, which primarily comprises Ni, Co and a minor quantity of Ca, Mg, Cu, Zn, Al and other impurities. The

(Received April 20, 2024; accepted June 24, 2024)

Published online: 10 July 2024

scarcity of surface water and the harsh natural environment in the Xinjiang region make it difficult to implement a complex and energy-intensive resource recycling mode, which results in the discarding of significant quantities of nickel and cobalt slag materials. If these solid wastes are not properly treated, it will lead to a waste of resources.[11,12] At the same time, it will seriously restrict the development of the mining industry and cause serious damage to the surrounding ecological environment. Recycling of these solid wastes is one of the ways to solve the problems of mineral resource scarcity and environmental pollution.[13,14] Therefore, effective recycling methods must be established to ensure the long-term sustainability of the lithium-ion battery supply chain.

Currently, hydrometallurgy and pyrometallurgy are the two main technologies for recovering valuable metals from solid waste resources.[15] Pyrometallurgy consumes large amounts of energy and emits harmful gases, causing serious environmental problems.[16] Compared with pyrometallurgy, hydrometallurgy plays an increasingly important role in resource recycling due to its advantages of low environmental pollution, low energy consumption and low requirements for equipment. The traditional utilization mode of hydrometallurgy is pre-treatment of solid waste, leaching and separation of each metal ion using solvent extraction, chemical precipitation, electrolysis and other methods. Leaching is a critical step in this process.[17,18] Inorganic acids such as H_2SO_4,[19] HCl,[20] HNO_3,[21] H_3PO_4[22] and organic acids such as citric acid and oxalic acid[23] have been widely used for the leaching of Ni and Co from spent batteries. However, the dissolution of nickel and cobalt requires a large amount of strong acid, resulting in equipment corrosion and high recovery costs, and the acidic leach solution with low pH has a greater impact on the environment and higher wastewater treatment costs.[24] In addition, most of the metal ions can be dissolved in acidic solution, and it is necessary to carry out a series of complicated in-depth decontamination processes such as copper removal, iron removal, magnesium removal, calcium removal, etc., and then a series of complicated processes such as pH regulation, extraction and separation, chemical precipitation, etc., repeatedly to obtain the leach solution with low impurity content.[25]

Ammonia leaching is also a commonly utilized technique in hydrometallurgy. Compared to the acid leaching method, ammonia leaching exhibits reduced leaching efficiency and a longer reaction time. Additionally, ammonia is a volatile substance, and the volatile ammonia gas has an irritating odor, which increases the absorption load of ambient gas and the requirements for equipment.[26,27] However, ammonia is considered a green leaching agent because of its low toxicity, low cost, recoverability and recyclability.[28] Ammonia leaching has also received much attention for its selectivity. Ni, Co, Cu, etc., can form complexes with ammonia and be leached selectively. Unwanted metals (such as Al, Ca and Fe) are hardly leached because of their poor ability to complex with ammonia. This can significantly reduce the process of removing impurities from the leach solution.[29] Ammonia leaching has been applied to extract and recover valuable metals from both ores and spent batteries.[30,31] Zheng et al.[32] employed ammonia, ammonium sulfate and sodium sulfite as leaching agents to recover valuable metals from lithium-ion waste batteries. This approach enabled the selective leaching of Li, Ni and Co, while Mn was precipitated and separated as $(NH_4)_2Mn(SO_3)_2$-H_2O. Yang et al.[33] employed an ammonia leaching process in the $(NH_4)_2CO_3$-NH_3-O_2 system to selectively extract approximately 98% of Ni and Co from spent batteries. The researchers then proceeded to achieve Ni and Co separation by solvent extraction. Ammonia can be evaporated and reused, reducing costs and avoiding the generation of high-salt wastewater. Tian et al.[34] applied ammonia leaching to selectively leach cobalt from high silica, low-grade cobalt ores in Africa, with a cobalt leaching rate of 95.61%. This process suppressed the leaching of other impurities and simplified the decontamination process. Moreover, among the many methods reported for the preparation of NCM cathode materials, hydroxide co-precipitation has been widely used in industrial production because of the advantages of homogeneous mixing, high crystallinity of the product and the fact that the morphology and size distribution of the precursor do not change significantly during the roasting process.[35,36] With alkaline leaching and alkaline co-precipitation, the two processes can be better combined with each other. It can realize the materialization of solid waste, shorten the process flow and reduce the discharge of saline wastewater.

In this study, a nickel and cobalt slag from a smelter was used to recover Ni and Co. An ammonia leaching method for recovering valuable metals from nickel and cobalt solid wastes was demonstrated, which provides an idea for the recovery and materialization of nickel and cobalt solid waste resources. The ammonia leaching system consists of $NH_3{\cdot}H_2O$-$(NH_4)_2SO_3$. $NH_3{\cdot}H_2O$ and NH_4^+ work together to increase free NH_3. They form a relatively stable buffer system to maintain the stability of the pH of the leaching system. The introduction of the reducing agent SO_3^{2-} can reduce the high-valent ions, which is conducive to enhancing the leaching of metals. This study investigated the factors that influence the leaching process, including the composition of the leaching solution, the concentration of each component, the liquid–solid ratio, time and temperature. The study also analyzed the leaching thermodynamics and kinetics of each metal to understand the feasibility of leaching, apparent activation energy of the leaching behavior

and control steps. This analysis provides a foundation for further enhancing leaching and optimizing the process.

EXPERIMENTAL

Materials

NCS was provided by a smelter in Xinjiang, China. Its main metal elements are Ni, Co and a small amount of Mn, Mg, Ca, Cu, etc. NCS was dissolved with concentrated hydrochloric acid, and its elemental composition and content were measured as shown in Table I. In this study, HCl, $NH_3{\cdot}H_2O$ and $(NH_4)_2SO_3{\cdot}H_2O$ were purchased from Sinopharm Group Co., Ltd, China. All chemicals used were analytically pure and solutions and the solutions used were made up of deionized water.

Leaching Experiments

The brief recycling of Ni and Co from NCS was presented in Fig. 1. NCS was ground in a mortar, sieved through a 100-mesh sieve and then used for leaching experiments. The ammonia leaching experiments for NCS were carried out in 100-mL round-bottom flasks placed in an oil bath equipped with a magnetic stirrer and temperature controller. The mouth of the flask was sealed with a glass stopper to avoid evaporation of the solution. The solution used as a leaching agent consists of $NH_3{\cdot}H_2O$, $(NH_4)_2SO_3{\cdot}H_2O$ and deionized water. The optimal process conditions, including $NH_3{\cdot}H_2O$ concentration, $(NH_4)_2SO_3{\cdot}H_2O$ concentration, L/S ratio, temperature and time, were determined through single trial experiments. The concentration of each metal ion in the leach solution was measured using ICP-AES. The leaching efficiency of each metal ion was calculated by Eq. 1:

$$x_i = \frac{c_i \times v}{m \times \omega_i} \times 100\% \quad (1)$$

where x_i and c_i (g/L) are the leaching rate and the concentration of element "i," respectively, V(L) is the volume of leachate, m(g) is the mass of NCS, and ω_i is the mass content of element "i" in the raw material.

Characterization

The elemental composition and content of the leach solution were measured by ICP-OES (PerkinElmerAvio500, Singapore). The physical structure of the solid samples was analyzed by XRD (Bruker D8 Advance, Germany). The valence states and their changes before and after NCS leaching were studied by XPS (Thermofisher K-Alpha, USA), and the spectral data were corrected according to the binding energy of C1s (284.8 eV). Thermodynamic analyses were carried out using E-pH diagrams.

RESULTS AND DISCUSSION

Thermodynamic Analysis

E-pH diagram is a thermodynamic equilibrium diagram used to show the tendency of a reaction or the range of stable phases present. It can provide a theoretical basis for leaching processes.[37] Therefore, the distribution of Ni, Co species in ammoniacal solutions was analyzed using E-pH diagrams to investigate the thermodynamic feasibility of using ammonia to leach Ni, Co.

Under standard conditions (298.15 K, 101.3 KPa), the possible species and equilibrium reactions in the system were determined, and the equilibrium line was calculated according to Eqs. 2 and 3. E-pH diagrams were plotted for the Ni-NH_3-H_2O and Co-NH_3-H_2O systems, respectively. The relevant data are shown in Tables II and III. Figure 2 illustrates that the hydrolysis pH of Ni and Co increases in the ammonia solution because of the formation of $[Ni(NH_3)_n]^{2+}$ and $[Co(NH_3)_n]^{2+}$. This greatly expands the stabilization zone of Ni and Co in the solution, which facilitates their leaching.

$$\Delta_r G_m^\theta = \Sigma\Delta_f G^\theta(\text{Reactants}) - \Sigma\Delta_f G^\theta(\text{Products}) \quad (2)$$

$$\Delta_r G_m^\theta = -nE^\theta F = RT\ln K \quad (3)$$

where $\Delta_r G_m{}^\theta$ is standard Gibbs energy change; R is ideal gas constant (8.314 J/K mol); T is temperature (K); K is equilibrium constant; $\Delta_f G^\theta$ is the standard generation Gibbs free energy.

Although Co^{3+} can form ammonium complexes in ammoniacal solutions where dissolution is thermodynamically possible, the dissolution kinetics are slow.[38] To facilitate the reaction, the addition of a reducing agent is required. Furthermore, Fig. 3

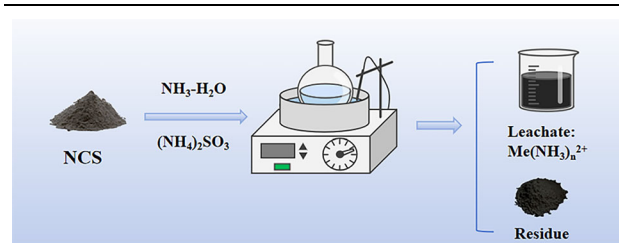

Fig. 1. Brief flowchart of recycling Ni and Co from NCS.

Table I. Element composition and concentration in NCS

Element	Ni	Co	Mn	Ca	Mg	Cu	Ba	Fe	Zn	Al
Content (%)	26.02	2.16	0.18	3.18	1.54	0.16	0.014	0.015	0.018	0.016

Table II. $\Delta_f G_m^\theta$ of substances of the Ni-NH_3-H_2O and Co-NH_3-H_2O system

Substance	State	$\Delta_f G_m^\theta$(kJ/mol)	Substance	State	$\Delta_f G_m^\theta$(kJ/mol)
H_2O	l	− 237.1	$[Ni(NH_3)_2]^{2+}$	aq	− 126.0
NH_3	l	− 26.5	$[Ni(NH_3)_3]^{2+}$	aq	− 164.1
H^+	l	0	$[Ni(NH_3)_4]^{2+}$	aq	− 197.3
Ni	s	0	$[Ni(NH_3)_5]^{2+}$	aq	− 228.2
Ni^{2+}	aq	− 45.63	$[Ni(NH_3)_6]^{2+}$	aq	− 255.7
$Ni(OH)_2$	s	− 458.9	$[Co(NH_3)]^{2+}$	aq	− 93.09
Co	s	0	$[Co(NH_3)_2]^{2+}$	aq	− 138.84
Co^{2+}	aq	− 54.51	$[Co(NH_3)_3]^{2+}$	aq	− 161.87
$Co(OH)_2$	s	− 454.4	$[Co(NH_3)_4]^{2+}$	aq	− 192.84
$Co(OH)_3$	s	− 596.61	$[Co(NH_3)_5]^{2+}$	aq	− 220.8
$[Ni(NH_3)]^{2+}$	aq	− 85.9	$[Co(NH_3)_6]^{2+}$	aq	− 243.99

Table III. Equilibrium constants for the complexation reaction of the Ni-NH_3-H_2O and Co-NH_3-H_2O system

Chemical reaction	Log k	Chemical reaction	Log k
$Ni^{2+} + NH_3 = [Ni(NH)_3]^{2+}$	2.8	$Co^{2+} + 4NH_3 = [Co(NH_3)_4]^{2+}$	5.55
$Ni^{2+} + 2NH_3 = [Ni(NH_3)_2]^{2+}$	5.04	$Co^{2+} + 5NH_3 = [Co(NH_3)_5]^{2+}$	5.73
$Ni^{2+} + 3NH_3 = [Ni(NH_3)_3]^{2+}$	6.77	$Co^{2+} + 6NH_3 = [Co(NH_3)_6]^{2+}$	5.11
$Ni^{2+} + 4NH_3 = [Ni(NH_3)_4]^{2+}$	7.96	$Co^{3+} + NH_3 = [Co(NH)_3]^{3+}$	6.70
$Ni^{2+} + 5NH_3 = [Ni(NH_3)_5]^{2+}$	8.71	$Co^{3+} + 2NH_3 = [Co(NH_3)_2]^{3+}$	14.00
$Ni^{2+} + 6NH_3 = [Ni(NH_3)_6]^{2+}$	8.74	$Co^{3+} + 3NH_3 = [Co(NH_3)_3]^{3+}$	20.10
$Co^{2+} + NH_3 = [Co(NH)_3]^{2+}$	2.11	$Co^{3+} + 4NH_3 = [Co(NH_3)_4]^{5+}$	25.70
$Co^{2+} + 2NH_3 = [Co(NH_3)_2]^{2+}$	3.74	$Co^{3+} + 5NH_3 = [Co(NH_3)_5]^{3+}$	30.80
$Co^{2+} + 3NH_3 = [Co(NH_3)_3]^{2+}$	4.79	$Co^{3+} + 6NH_3 = [Co(NH_3)_6]^{3+}$	35.20

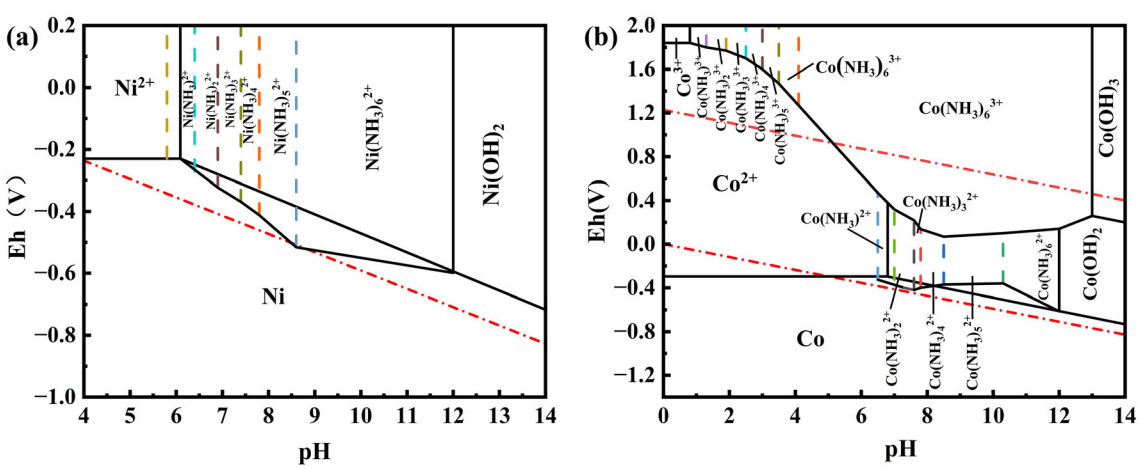

Fig. 2. E-pH diagram: (a) Ni-NH_3-H_2O system; (b) Co-NH_3-H_2O system (25°C, $[NH_3]$ = 4 mol/L, $[Ni^{2+}]$ = 1 mol/L, $[Co^{2+}]$ = 0.1 mol/L).

shows that the presence of ammonia alone results in a high pH, which is unfavorable for the stable existence of metal-ammonia complexes. However, the introduction of $(NH_4)_2SO_3$ significantly reduces the pH of the system, making it favorable for the leaching of Ni and Co. $(NH_4)_2SO_3$ also inhibits the dissociation of ammonia into NH_4^+ and OH^-, thereby increasing the concentration of free NH_3. Thus, the ideal leaching system should comprise $NH_3{\cdot}H_2O$, NH_4^+ and a reducing agent.

In conclusion, the presence of ammonia solution enables the conversion of nickel and cobalt into complexes with ammonia, thus facilitating their leaching. $(NH_4)_2SO_3$ and $NH_3{\cdot}H_2O$ provide free NH_3 and form a buffer solution to maintain the pH stability of the system, thereby ensuring that the

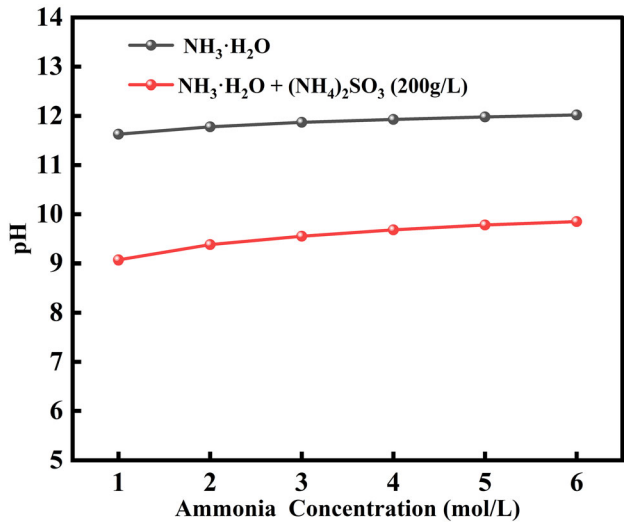

Fig. 3. pH of different leaching systems.

pH of the system falls within the range where $[Ni(NH_3)_n]^{2+}$ and $[Co(NH_3)_n]^{2+}$ are present. $(NH_4)_2SO_3$ reduces Ni^{3+} and Co^{3+} and enhances the leaching efficiency. The leaching system described in this study is thermodynamically feasible.

Leaching Conditions

Effect of $NH_3{\cdot}H_2O$ Concentration

The effect of the $NH_3{\cdot}H_2O$ concentration (1, 2, 3, 4, 5, 6 mol/L) on the leaching rate of nickel and cobalt has been studied under the following conditions: temperature of 60°C, L/S ratio of 10 mL/g, 250 g/L $(NH_4)_2SO_3{\cdot}H_2O$ and leaching time of 90 min. The result is shown in Fig. 4a. As the concentration of $NH_3{\cdot}H_2O$ increases, the leaching rate of Ni and Co also increases. However, when the $NH_3{\cdot}H_2O$ concentration exceeds 4 mol/L, the leaching rate increases at a slower rate and eventually stabilizes. The increase in ammonia concentration also leads to an increase in the pH value and vapor pressure of the solution, resulting in higher leaching costs and reduced stability of the leaching system. Based on the given factors, it was determined that the optimal ammonia concentration for the leaching system is 4 mol/L.

Effect of $(NH_4)_2SO_3{\cdot}H_2O$ Concentration

Under the leaching conditions of 60°C, L/S ratio of 10 mL/g, $NH_3{\cdot}H_2O$ concentration of 4 mol/L and leaching time of 90 min, the effects of different $(NH_4)_2SO_3{\cdot}H_2O$ concentrations on the leaching rate of Ni and Co were investigated. As shown in the Fig. 4b, the leaching efficiency of Ni and Co was significantly improved by the addition of $(NH_4)_2SO_3{\cdot}H_2O$. This is due to the buffer system formed by $(NH_4)_2SO_3{\cdot}H_2O$ and $NH_3{\cdot}H_2O$, which helps maintain the pH stability of the system. The pH of the solution can be calculated using Eq. 5. $(NH_4)_2SO_3{\cdot}H_2O$ can inhibit the dissociation of $NH_3{\cdot}H_2O$ (Eq. 4) and increase the concentration of free NH_3 in solution. This, in turn, can increase the possibility of metal ions complexing with NH_3 in solution. On the other hand, the introduction of the reducing agent SO_3^{2-} can reduce the trivalent Ni, Co in the slag material and strengthen the leaching of metals. When the concentration of $(NH_4)_2SO_3{\cdot}H_2O$ exceeded 225 g/L, the leaching efficiency basically remained stable. This is because SO_3^{2-} is in the state of excess, and when the complexation ability of NH_3 with metal ions reaches saturation, continuing to increase the concentration of $(NH_4)_2SO_3{\cdot}H_2O$ has little effect on improving the leaching rate. The concentration of $(NH_4)_2SO_3{\cdot}H_2O$ was set at 225 g/L.

$$NH_3 \cdot H_2O \leftrightharpoons NH_4^+ + OH^- \tag{4}$$

$$pH = pK_a + \log\left([NH_3]/NH_4^+\right) \tag{5}$$

Effect of L/S Ratio

The effect of the L/S ratio on the leaching efficiency can be seen in Fig. 4c. As the L/S ratio increases from 2 mL/g to 5 mL/g, the leaching rate increases rapidly. This is due to the increase in solution volume, which facilitates the diffusion of metal in the powder. Additionally, the contact area between the solid particles and the liquid also increases, promoting the leaching of the metal. The leaching rate remains stable when the L/S ratio exceeds 5 mL/g. Therefore, the leaching L/S ratio is set at 5 mL/g.

Effect of Time and Temperature

Under the experimental conditions described above, the effect of time and temperature on the leaching rate of Ni and Co was investigated. The results indicate that an increase in temperature and time had a positive effect on the leaching process of both Ni and Co, as illustrated in the Fig. 4d and e. Appropriate warming can speed up leachate filtration. This is because higher temperatures decrease the viscosity of the solution, reducing resistance to filtration and increasing the filtration rate. However, it is important to note that ammonia is volatile, and its volatility increases with temperature. The volatilization of ammonia results in the loss of ammonia and increases the load of ambient gas absorption, which is not favorable for industrial production. When the leaching time exceeds 45 min and the temperature exceeds 55°C, the leaching rate of Ni and Co basically tends to stabilize, indicating that the leaching system is basically reacted completely under these conditions.

According to the analysis above, the optimal leaching process conditions were as follows:

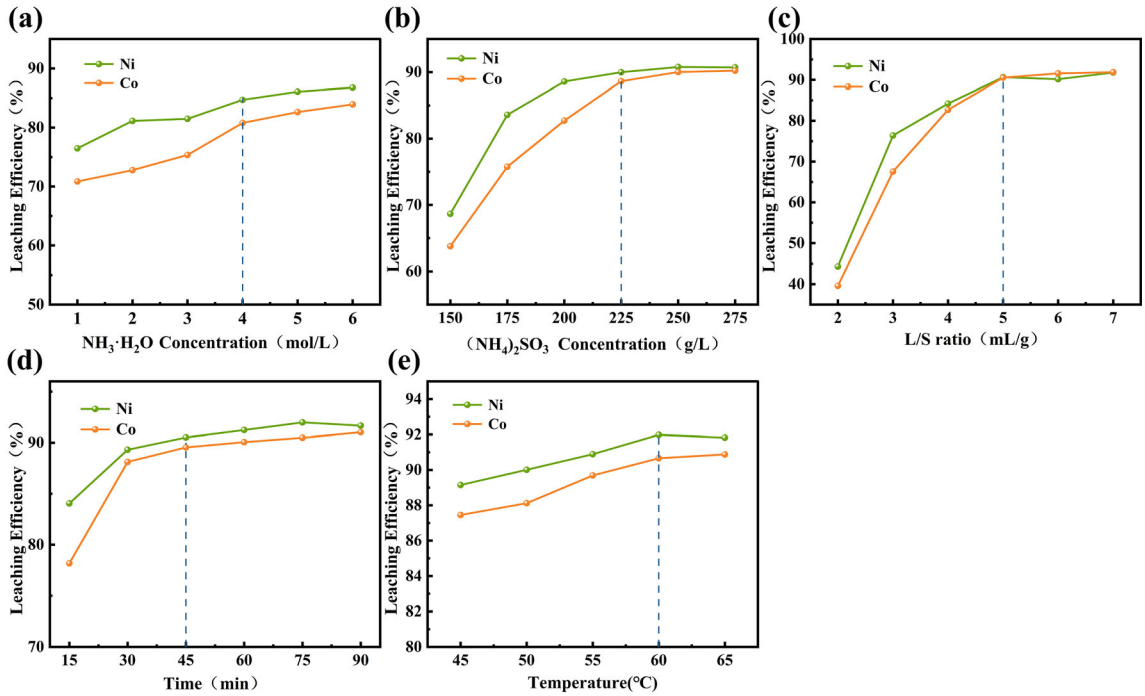

Fig. 4. Effects of (a) $NH_3{\cdot}H_2O$ concentration, (b) $(NH_4)_2SO_3{\cdot}H_2O$ concentration, (c) L/S ratio, (d) time, (e) temperature on leaching efficiency.

Table IV. Element composition and concentration in leaching solution

Element	Ni	Co	Mn	Ca	Mg	Cu
Concentration (g/L)	48.45	4.01	0.2	0.031	0.01	0.16

$NH_3{\cdot}H_2O$ concentration of 4 mol/L, $(NH_4)_2SO_3{\cdot}H_2O$ concentration of 225 g/L, L/S ratio of 5 mL/g, leaching time of 45 min and temperature of 55°C. Table IV presents the elemental composition and content of the leach solution. The types and contents of impurity ions were reduced, and the leaching system exhibited selectivity for Ni and Co. The leach solution is a Ni-Co-NH_3-H_2O system, which is consistent with the system used for the preparation of NCM ternary precursors by co-precipitation. Therefore, the leachate can be subsequently used for the synthesis of NCM ternary precursors.

Kinetics Analysis

Under the optimal experimental conditions, the variation of the leaching rate of Ni and Co with time was monitored at different temperatures (45–60°C) to analyze the reaction kinetics of the leaching process. The results are shown in Fig. 5.

The reductive ammonia leaching of NCS is a liquid-solid reaction that occurs between the solid and fluid phases. The common model used to simulate multiple liquid-solid reactions is unreacted shrinking core model (USCM). It can be expressed as (a) surface chemical reaction control model and (b) diffusion control model.[39,40] During the leaching process, the concentration of the leaching agent changes over time. NCS contains various metals such as Ni, Co, Mg, Ca, Cu and Zn, making the leaching behavior complex. Additionally, the leaching process involves redox reactions. To accurately describe the leaching process of NCS, (c) logarithmic model is used.[41] The empirical model is frequently used to describe the study of chemical reaction kinetics.

$$(a): 1-(1-X)^{1/3} = k_1 t \tag{6}$$

$$(b):\ 1-2X/3-(1-X)^{\frac{2}{3}} = k_2 t \tag{7}$$

$$(c): (-\ln(1-X))^2 = k_3 t \tag{8}$$

where k is the reaction rate constant (min^{-1}), x is the leaching efficiency (%) of different metals, and t is the reaction time (min). The fitting results are

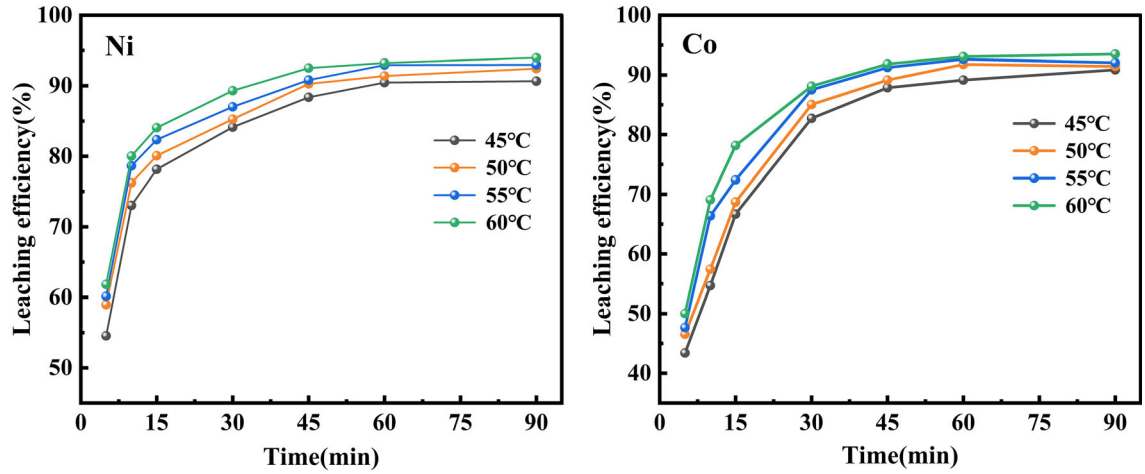

Fig. 5. Leaching efficiency of Ni and Co for different temperatures.

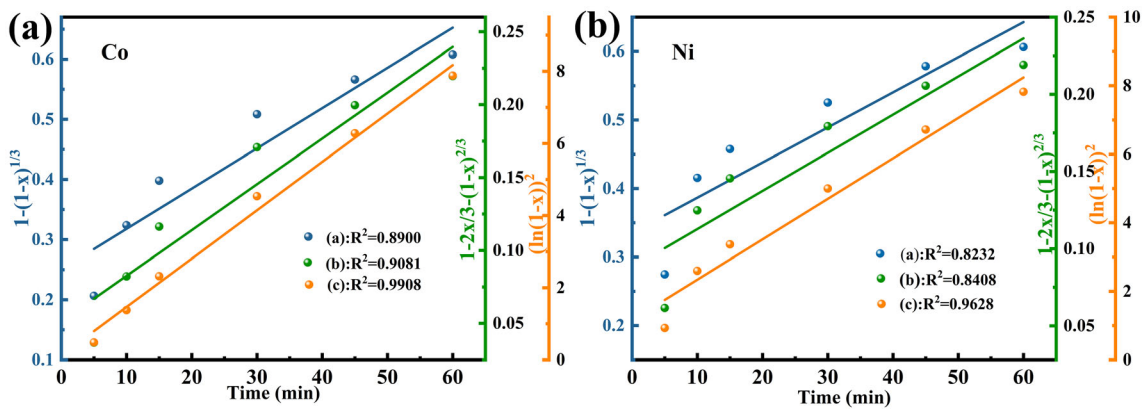

Fig. 6. Fitting plots of different models at 60°C.

shown in Fig. 6. The results show that $(-\ln(1-x))^2$ has a better linear relationship with time compared to the shrinkage unresponsive model. Accordingly, the logarithmic law model (Eq. 8) was employed to describe the leaching behavior of Ni and Co.

To determine the control steps of the leaching process and the apparent activation energy, Arrhenius Eqs. 9 and 10. were used to express the relationship between k and T:

$$K = Ae^{-E_a/RT} \tag{9}$$

$$\ln K = \ln A - E_a/RT \tag{10}$$

The Arrhenius plots were fitted using 1000/T as the horizontal coordinate and ln k as the vertical coordinate. The results of the fitting are shown in Fig. 7. The slopes of the Arrhenius plots for Ni and Co were − 2.4289 and − 2.6456, respectively. This allowed for the calculation of the apparent activation energies of Ni and Co, which were found to be 20.19 kJ/mol and 22.00 kJ/mol, respectively. As described in the relevant literature, the reaction is controlled by diffusion when the apparent activation energy is < 30 kJ/mol.[42] Therefore, under the analysis of the logarithmic law model, the activation energies for the leaching of Ni and Co were 20.19 kJ/mol and 22.00 kJ/mol, respectively. The leaching reaction was found to be diffusion controlled. In accordance with the characteristics of a diffusion-controlled reaction, the effect of temperature on the leaching efficiency was found to be minimal, which is consistent with the experimental results. According to the characteristics of a diffusion-controlled reaction, the effect of temperature on the leaching efficiency was found to be minimal, which is consistent with the experimental results.

Characterization Analysis

XRDs were carried out on the NCS used in the experiments, and it can be seen from Fig. 8a that the NCS contains $NiSO_4$, $Ni(OH)_2$ and some impurities such as Ca , Al and Mg. The XRD profile peaks of NCS are complex. This is due to the large variety of impurities in this raw material and the poor crystallinity of the sample after washing and mechanical mixing steps in the preparation process, making the components more difficult to

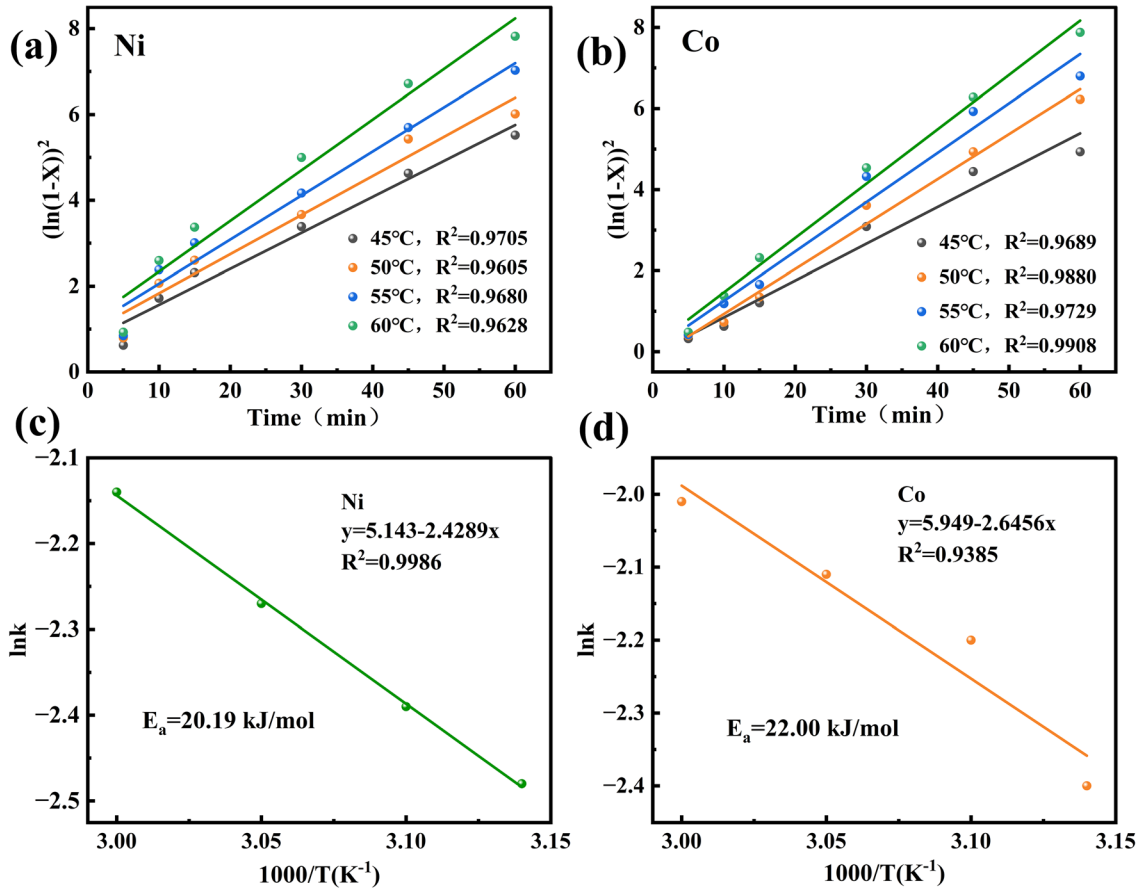

Fig. 7. (a) Ni, (b) Co based on $(-\ln(1-x))^2$ kinetic fitting results; Arrhenius plot of lnk-1000/T for (c) Ni, (d) Co based on the log rate law model.

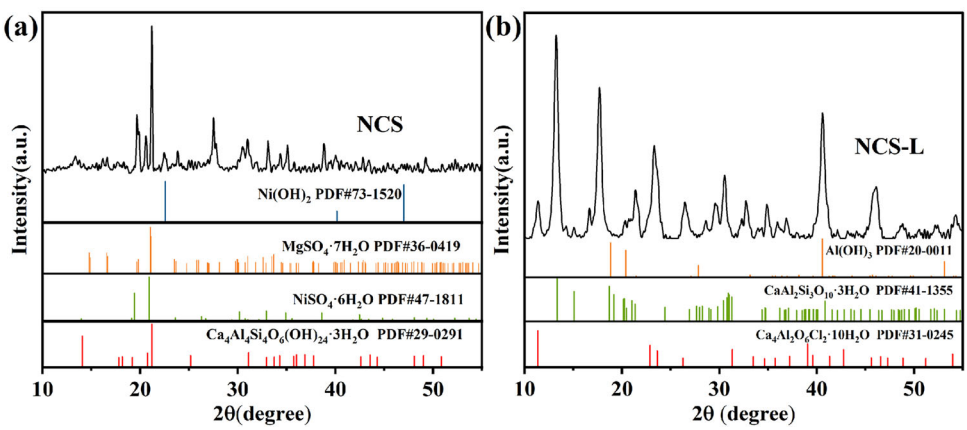

Fig. 8. XRD patterns of (a) NCS (b) NCS-L.

distinguish. However, NCS is a precipitate produced by the oxidation of precipitated Co^{2+} by NiOOH, and the chemical equation for the reaction is shown in Eq. 11. Theoretically, NCS should contain NiOOH, CoOOH, Ni^{2+}, Co^{2+} and other impurity ions. Figure 7b presents the XRD pattern of the leaching residue (NCS-L), which is dominated by impurities such as Al, Ca, etc., indicating that Ni and Co are leached out of solution, while Ca, Al, etc., are unable to complex with ammonia and remain in the residue.

$$\mathrm{NiOOH} + \mathrm{Co}^{2+} = \mathrm{CoOOH} + \mathrm{Ni}^{2+} \qquad (11)$$

The valence states of Ni and Co in NCS and NCS-L were analyzed by XPS. The XPS spectrum of Ni 2p is shown in Fig. 9a. In NCS, the Ni 2p3/2 peak has two split peaks located at 855.74 eV and 857.85 eV, corresponding to Ni^{2+} and Ni^{3+}, respectively.[43,44]

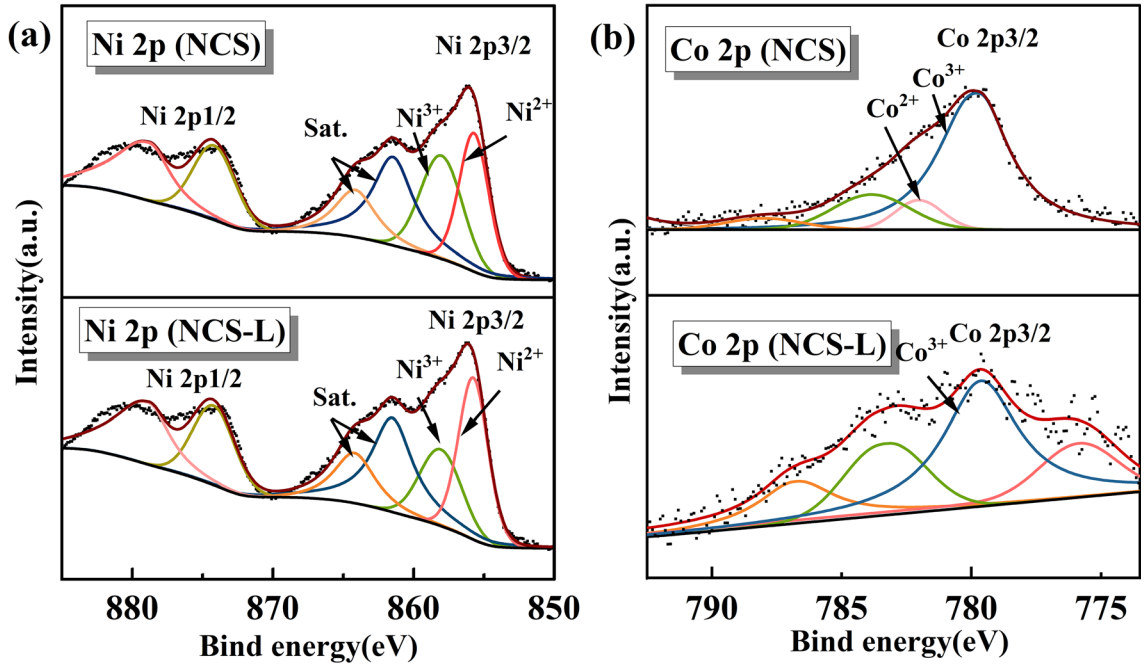

Fig. 9. XPS patterns of (a) Ni 2*p* (b) Co 2*p*.

For NCS-L, there was a significant increase in the Ni^{2+}/Ni^{3+}, which could be attributed to the reduction of Ni^{3+} to Ni^{2+} in the presence of $(NH_4)_2SO_3$. Figure 9b shows the XPS spectrum of Co 2*p*. In the NCS, the Co 2*p*3/2 orbitals are mainly composed of 779.41 eV and 781.37 eV peaks, corresponding to Co^{3+} and Co^{2+}, respectively.[12,45,46] After leaching, the Co content in NCS-L was less, the Co^{2+} fractional peak at 781.37 eV disappeared, and the Co^{3+} content also decreased. Based on the above analyses, Ni and Co were present in both 2- and 3-valent states in NCS, while Ni^{3+} and Co^{3+} were reduced in NCS-L. It was postulated that the following reactions occurred during the leaching process (Me = Ni, Co):

$$2MeOOH + SO_3^{2-} = 2MeO + SO_4^{2-} + H_2O$$

$$MeO + nNH_3 + H_2O = Me(NH_3)_n^{2+} + 2OH^-$$

$$Me(OH)_2 + nNH_3 + 2H^+ = Me(NH_3)_n^{2+} + 2H_2O$$

$$Me^{2+} + nNH_3 = Me(NH_3)_n^{2+}$$

CONCLUSION

This study presents a reductive ammonia leaching method for extracting Ni and Co from nickel-cobalt solid waste. The leaching process is described in detail, and the results indicate that a reducing agent is necessary because of the presence of Ni^{3+} and Co^{3+}. $(NH_4)_2SO_3$ can effectively reduce and enhance the leaching process. Additionally, we conducted a systematic investigation into the impact of leaching parameter conditions on metal leaching efficiency. Under the optimized conditions of ammonia concentration of 4 mol/L, $(NH_3)_2SO_3$ concentration of 225 g/L, liquid-solid ratio of 5 mL/g, time of 45 min and temperature of 60°C, the leaching efficiency of nickel and cobalt reached 90.09% and 89.24%, respectively. The types and contents of impurities in the leach solution were significantly reduced. The method is selective and can simplify the subsequent decontamination process. The kinetic results indicate that the leaching process is diffusion controlled, and the activation energies for the leaching of Ni and Co were 20.19 kJ/mol and 22.00 kJ/mol, respectively. This paper proposes the wet leaching method for simultaneous leaching of Ni and Co from nickel and cobalt slag material. The resulting Ni and Co in the leach solution can be separated to prepare products or directly materialized to prepare high value-added products such as NCM.

ACKNOWLEDGEMENTS

This work was supported by National Natural Science Foundation of China (U1903217).

CONFLICT OF INTEREST

The authors declare that they have no conflict of interest.

REFERENCES

1. X. Zhang, L. Li, E. Fan, Q. Xue, Y. Bian, F. Wu, and R. Chen, *Chem. Soc. Rev.* 47, 7239 https://doi.org/10.1039/c8cs00297e (2018).
2. T. Kim, W. Song, D.-Y. Son, L.K. Ono, and Y. Qi, *J. Mater. Chem. A* 7, 2942 https://doi.org/10.1039/c8ta10513h (2019).
3. Y. Hua, X. Liu, S. Zhou, Y. Huang, H. Ling, and S. Yang, *Resour. Conserv. Recycl.* 168, 105249 https://doi.org/10.1016/j.resconrec.2020.105249 (2020).
4. J. Shan, M. Deying, L. Ziang, L. Ruhong, L. Zhu, W. Yue, T. Shuang, and D. Changsong, *J. Clean. Prod.* 340, 130535 https://doi.org/10.1016/j.jclepro.2022.130535 (2022).
5. Z. Zhicheng, T. Jinfeng, S. Minhua, X. Junhua, and S. Kaimin, *ACS Sustain. Chem. Eng.* 11, 16124 https://doi.org/10.1021/acssuschemeng.3c03797 (2023).
6. J. Song, F. Ning, Y. Zuo, A. Li, H. Wang, K. Zhang, T. Yang, Y. Yang, C. Gao, W. Xiao, Z. Jiang, T. Chen, G. Feng, and D. Xia, *Adv. Mater.* 35, 2208726 https://doi.org/10.1002/adma.202208726 (2022).
7. C. Zhuangzhuang, L. Xiao, B. Xiaoyu, R. Xiaodi, and O. Xing, *Energy Storage Mater.* 57, 14 https://doi.org/10.1016/j.ensm.2023.02.003 (2023).
8. C. Han, Y. Cao, S. Zhang, L. Bai, M. Yang, S. Fang, H. Gong, D. Tang, F. Pan, Z. Jiang, and J. Sun, *Small* 19, 2207453 https://doi.org/10.1002/smll.202207453 (2023).
9. D. Peralta, J. Salomon, J.-F. Colin, A. Boulineau, F. Fabre, C. Bourbon, B. Amestoy, E. Gutel, D. Bloch, and S. Patoux, *J. Power Sources* 396, 527 https://doi.org/10.1016/j.jpowsour.2018.06.075 (2018).
10. Q. Li, K.Y. Fung, and K.M. Ng, *ACS Sustain. Chem. Eng.* 7, 12718 https://doi.org/10.1021/acssuschemeng.9b00590 (2019).
11. Y. Lou, X. Tang, C. Liu, and W. Zhang, *JOM* 75, 381 https://doi.org/10.1007/s11837-022-05530-7 (2022).
12. Y. Wang, Z. Xu, X. Zhang, E. Yang, and Y. Tu, *Sep. Purif. Technol.* 299, 121782 https://doi.org/10.1016/j.seppur.2022.121782 (2022).
13. Q. Hu, Z. Luo, H. Zhou, and Z. Cao, *Waste Manag.* 167, 204 https://doi.org/10.1016/j.wasman.2023.05.045 (2023).
14. G. Pei, Y. Peng, Y. Tian, Z. Xiaolan, and S. Boxiong, *J. Energy Storage* 68, 107652 https://doi.org/10.1016/j.est.2023.107652 (2023).
15. X. Zheng, W. Gao, X. Zhang, M. He, X. Lin, H. Cao, Y. Zhang, and Z. Sun, *Waste Manag.* 60, 680–688 https://doi.org/10.1016/j.wasman.2016.12.007 (2016).
16. L. Chunyan, D. Guofu, L. Runyu, W. Chen, W. Sheng, J. Yue, J. Haishen, J. Shaojun, and D. Chenlong, *Sep. Purif. Technol.* 306, 233611 https://doi.org/10.1016/j.seppur.2022.122559 (2022).
17. Y. Ma, J. Tang, R. Wanaldi, X. Zhou, H. Wang, C. Zhou, and J. Yang, *J. Hazard. Mater.* 402, 123491 https://doi.org/10.1016/j.jhazmat.2020.123491 (2020).
18. J.C.-Y. Jung, P.-C. Sui, and J. Zhang, *J. Energy Storage* 35, 102217 https://doi.org/10.1016/j.est.2020.102217 (2021).
19. Y. Yang, S. Lei, S. Song, W. Sun, and L. Wang, *Waste Manag.* 102, 131 https://doi.org/10.1016/j.wasman.2019.09.044 (2019).
20. Z. Takacova, T. Havlik, F. Kukurugya, and D. Orac, *Hydrometallurgy* 163, 9 https://doi.org/10.1016/j.hydromet.2016.03.007 (2016).
21. A. Marouane, H. Rachid, L. Clément, T. Yassine, G. Abdellatif, R. Jérôme, and S. Ismael, *J. Power Sources* 580, 233341 https://doi.org/10.1016/j.jpowsour.2023.233341 (2023).
22. G. Li, Q. Zhou, Z. Zhu, J. Luo, M. Rao, Z. Peng, and T. Jiang, *J. Clean. Prod.* 189, 620 https://doi.org/10.1016/j.jclepro.2018.04.083 (2018).
23. J. Yunjai, H. Chia-Hung, K. Kyungjung, K. Jin Soo, and C. Eunhyea, *Chemosphere* 317, 137865 https://doi.org/10.1016/j.chemosphere.2023.137865 (2023).
24. C. Wu, B. Li, C. Yuan, S. Ni, and L. Li, *Waste Manag.* 93, 153–161 https://doi.org/10.1016/j.wasman.2019.04.039 (2019).
25. D. Li, B. Zhang, L. Ye, Z. Xiao, L. Ming, and X. Ou, *J. Clean. Prod.* 349, 131373 https://doi.org/10.1016/j.jclepro.2022.131373 (2022).
26. L. Ye, H. Gong, B. Zhang, and X. Ou, *Sep. Purif. Technol.* 330, 125507 https://doi.org/10.1016/j.seppur.2023.125507 (2023).
27. K. Meng, Y. Cao, B. Zhang, X. Ou, D.-M. Li, J.-F. Zhang, and X. Ji, *ACS Sustain. Chem. Eng.* 7, 7750–7759 https://doi.org/10.1021/acssuschemeng.8b06675 (2019).
28. Y. Long, G. Haiqiang, Z. Bao, and O. Xing, *Sep. Purif. Technol.* 330, 125507 https://doi.org/10.1016/j.seppur.2023.125507 (2023).
29. Y. Cheng, Z. Jialiang, C. Yongqiang, and W. Chengyan, *J. Power Sources* 584, 233611 https://doi.org/10.1016/j.jpowsour.2023.233611 (2023).
30. C. Wang, S. Wang, F. Yan, Z. Zhang, X. Shen, and Z. Zhang, *Waste Manag.* 114, 253 https://doi.org/10.1016/j.wasman.2020.07.008 (2020).
31. S. Ilyas, R.R. Srivastava, H. Kim, N. Ilyas, and R. Sattar, *Sep. Purif. Technol.* 232, 115971 https://doi.org/10.1016/j.seppur.2019.115971 (2019).
32. X. Zheng, W. Gao, X. Zhang, M. He, X. Lin, H. Cao, Y. Zhang, and Z. Sun, *Waste Manag.* https://doi.org/10.1016/j.wasman.2016.12.007 (2016).
33. C. Yang, J. Zhang, Y. Chen, and C. Wang, *J. Power Sources* 584, 233611 https://doi.org/10.1016/j.jpowsour.2023.233611 (2023).
34. L. Tian, A. Gong, W. Xuangao, Y. Xiaoqiang, X. Zhifeng, and L. Chen, *Int. J. Miner. Metall. Mater.* 29, 218 https://doi.org/10.1007/s12613-020-2161-6 (2021).
35. K. Xiangbang, Y. Huiya, Z. Yige, D. Pengpeng, T. Yonglin, Z. Jing, and Z. Jinbao, *Chem. Eng. J.* 452, 139431 https://doi.org/10.1016/j.cej.2022.139431 (2022).
36. X. Yang, X. Huang, H. Shi, P. Dong, D. Wang, J. Duan, and Y. Zhang, *J. Energy Chem.* 53, 379–386 https://doi.org/10.1016/j.jechem.2020.05.049 (2020).
37. J. Yu, B. Ma, C. Wang, and Y. Chen, *Waste Manag.* 162, 92 https://doi.org/10.1016/j.wasman.2023.03.013 (2023).
38. H. Ku, Y. Jung, M. Jo, S. Park, S. Kim, D. Yang, K. Rhee, E.-M. An, J. Sohn, and K. Kwon, *J. Hazard. Mater.* 313, 2753 https://doi.org/10.1016/j.jhazmat.2016.03.062 (2016).
39. L. Li, Y. Bian, X. Zhang, Y. Guan, E. Fan, F. Wu, and R. Chen, *Waste Manag.* 71, 362 https://doi.org/10.1016/j.wasman.2017.10.028 (2017).
40. H. Zhou, Z. Luo, S. Wang, X. Ma, and Z. Cao, *Separ. Purif. Technol.* 315, 123742 https://doi.org/10.1016/j.seppur.2023.123742 (2023).
41. X. Chen, J. Li, D. Kang, T. Zhou, and H. Ma, *Green Chem.* 21, 6342 https://doi.org/10.1039/c9gc02844g (2019).
42. X. Zhou, W. Yang, X. Liu, J. Tang, F. Su, Z. Li, J. Yang, and Y. Ma, *Waste Manag.* 155, 53 https://doi.org/10.1016/j.wasman.2022.10.034 (2022).
43. B. Xue, J. Zengyan, S. Yanzhi, L. Xiaoguang, J. Xin, H. Rui, L. Zhenfa, and P. Junqing, *ACS Sustain. Chem. Eng.* 11, 3673 https://doi.org/10.1021/acssuschemeng.2c06630 (2023).
44. H. Qian, Z. Hong, and C. Zhanfang, *Sep. Purif. Technol.* 325, 124653 https://doi.org/10.1016/j.seppur.2023.124653 (2023).
45. D. Kochubey, V. Kaichev, A. Saraev, S. Tomyn, A. Belov, and Y. Voloshin, *J. Phys. Chem. C* 117, 2753 https://doi.org/10.1021/jp3085606 (2013).
46. L.K. Parrott and E. Erasmus, *Catal. Lett.* 148, 2008 https://doi.org/10.1007/s10562-018-2411-7 (2018).

Publisher's Note Springer Nature remains neutral with regard to jurisdictional claims in published maps and institutional affiliations.

Springer Nature or its licensor (e.g. a society or other partner) holds exclusive rights to this article under a publishing agreement with the author(s) or other rightsholder(s); author self-archiving of the accepted manuscript version of this article is solely governed by the terms of such publishing agreement and applicable law.